A New Image Super-Resolution Restoration Algorithm

Sayed A. Mohamed
Data Reception, Analysis and Receiving Station Affairs
National Authority for Remote Sensing and Space Sciences
Cairo, Egypt

A. S. El-Sherbeny
Department of Industrial Electronic Engineering and Control
Faculty of Electronic Engineering,
Menoufia University
Menoufia, Egypt

Ayman H. Nasr
Data Reception Analysis and Receiving Station Affairs
National Authority for Remote Sensing and Space Sciences
Cairo, Egypt

A. K. Helmy
Data Reception Analysis and Receiving Station Affairs
National Authority for Remote Sensing and Space Sciences
Cairo, Egypt

ABSTRACT

This paper proposes a new image super-resolution restoration algorithm. The development of the algorithm is based on the improvement of the classical projection onto convex set (POCS) algorithm and the stationary wavelet transform (SWT) to restore a super-resolution image from Egyptsat-1 low resolution (LR) images. Egyptsat-1 bands have inconsistent sub-pixel shift. this inconsistent shift between the bands is changed into reliable shift by adaptive interpolation. Then, decomposition of high frequency sub-bands is generated using (SWT). The POCS iteration is used to restore high-resolution (HR) image from every LR wavelet decomposed images. The HR image is reconstructed by inverse wavelet transform. The result showed that the proposed method achieved significant spatial resolution improvements from 7.8 m to 4 m by using (POCS). The reconstructed image is evaluated by several quantitative measures: the peak signal-noise ratio(PSNR), root main square error(RMSE), entropy, and Objective Fusion Measure. These measures of the proposed method were also assessed and tested with some implemented commonly used SR methods. The experimental results of the processed Egyptsat-1 images showed that the proposed method can improve the ability of fusing different image information, and the visual and quantitative evaluations verify its usefulness and effectiveness.

General Terms
Digital Image processing, Remote sensing

Keywords
Super-resolution; Projection on convex set; Stationary wavelet transforms; Egyptsat-1 images; Peak signal-noise ratio; Root main square error; Entropy; Objective fusion measure.

1. INTRODUCTION
Super Resolution Image Reconstruction (SRIR) is a method to reconstruct a high-resolution (HR) image using multi low-resolution (LR) images with the relative displacement or video sequences in the same scene. Super-resolution reconstruction method has been widely used in many fields including remote sensing, astronomy, military surveillance and medical diagnostics etc. With the development of information technology and sensor technology, many kinds of image sensors are being widely used. How to deal with the images from different sensors becomes a key research field. (SRIR), is a process to combine different information from several images into single image, highlights the useful information and the prominent feature of original images. The Egyptian satellite (Egyptsat-1) is the first earth observation satellite of Egypt. Some of its images have inconsistent sub-pixel shift [1], [2]. The general strategy that characterizes SR comprises three major processing steps: LR image registration or motion estimation, image interpolation and HR image reconstruction [3]. The conventional SR methods convert the SR reconstruction into a fusion problem by super-resolving an HR image via alignment and registration between a set of multi frame LR images [4]. Very high accuracy, (i.e., precise alignment) is essentially required in the registration (up to sub-pixel level) to be able to reconstruct the HR image correctly. The first point is the inconsistent shift between the Egyptsat-1 bands is transformed into reliable shift by adaptive interpolation to be correctly aligned with each other on a common grid. Thus, accurate knowledge of registration parameters is required for each of the input LR frames. The second point is to generate the high resolution (HR) image. A new resolution enhancement technique for digital images has been proposed in this work using a wavelet-domain based on (POCS) technique. In principle, multi-frame super-resolution techniques attempt to seek and combine high frequency information hidden in a group of low resolution frames, while the low frequency information contained in the reference frame should be essentially retained during the SR computation. From the multi-scale signal processing point of view, the high frequency information is contained in the wavelet coefficients which should be extended [5]. On the other hand, the low-frequency information is contained in the approximation coefficients which should be preserved. Based on this concept, we present a wavelet constrained POCS (SWT-POCS) technique. Instead of performing the POCS in the image domain itself, we update the wavelet coefficients in the LH, HL, and HH bands using the neighboring frames of the reference frame while keeping the low frequency band, the LL band, unchanged throughout the SR computation. The remainder of the paper is organized as follows:

Section2 describes the idea of transforming the inconsistent sub-pixel into reliable shift (image motion estimation). The stationary wavelet transforms and the principle of POCS super resolution are explained in section 3 and section 4 respectively. Section 5 describes the idea of the stationary wavelet constrained POCS super-resolution algorithm. Section 6 focuses on the data acquisition and the study area. The proposed methodology and the results are discussed in sections 7 and section 8 respectively. Section 9 depicted on the evaluation criteria. finally, the concluding remarks are given in section 10.

2. IMAGE MOTION ESTIMATION
In many super-resolution applications, fast pairwise image motion estimation and image registration (IR) are sufficient for estimation and registration the relative shifts between the sets of low-resolution images. To define motion estimation and IR, it is the process of covering two or more images of the same scene taken at different times, from different viewpoints and/or by different sensors [6]. Explicit motion estimation is a major factor

that affects the performance of the motion-based SR algorithm. The accuracy of SR algorithms is quite often limited by the ability to measure motion estimation and registration of low-resolution images [7][8]. In image motion estimation, the input images with irregularly spaced pixels need to be correctly aligned with each other on a common grid. Therefore, accurate knowledge of motion estimation parameters is required for each of the input LR frames. Accurate registration of images is the most fundamental component to high performance image processing techniques such as multi-frame image fusion, change detection, and super-resolution [9]. Miss-alignment of the LR frames will result in the reconstruction of an incorrect HR image. In fact, we estimate the relative motion estimation of pixels between the different images with fractional pixel accuracy, and then we combine together sampling points according to the estimated motion, to produce a single image plane. For fractional pixel accuracy, it is required to calculate the rotation between them to get the correct robust result [2], [10].

Register the observed low-resolution images to one another using a Frequency domain approach allows us to estimate the horizontal and vertical shift and the planar rotation separately from the most important frequencies of images. Given a reference image f_1 (x, y). Its shifted and rotated version f_2 (x, y) would be represented as follows:

$$f_2 (X) = f1 (R (X+\Delta X)), \qquad (1)$$

$$\text{With } X = \begin{bmatrix} x \\ y \end{bmatrix}, \qquad \Delta X = \begin{bmatrix} \Delta x \\ \Delta y \end{bmatrix}, \quad R = \begin{bmatrix} \cos\emptyset & -\sin\emptyset \\ \sin\emptyset & \cos\emptyset \end{bmatrix}$$

Where Δx the Horizontal shift Δy is the Vertical shift and R is the rotation angle $\emptyset$. In this case, the images will be measured for displacement and rotation angle. We followed Bernd Jähne, and Steven T. Karris application of the Fourier Transform properties on our measured images to calculate displacement and rotation angles [11], [12] as follows:

$$F_2(u) = \int \int_X f_2(X) \, e^{-j2\pi u^T X} \, dX$$
$$= \int \int_X f_1(R(X + \Delta X)) \, e^{-j2\pi u^T X} dX$$
$$= e^{j2\pi u^T \Delta X} \int \int_{X'} f_1(R\acute{x}) \, e^{-j2\pi u^T X} \, d\acute{X} \qquad (2)$$

Which depend on the shifts and is a rotated version of $|F_1(u)|$. It is therefore possible to estimate the relative rotation angle between two images of the Egyptsat-1 mismatch bands, then apply the inverse rotation to the Fourier transform. The phase shift can be computed from the resulting image and the reference image [13].

3. STATIONARY WAVELET TRANSFORMS (SWT)

The wavelet transform has become a popular image representation in recent years. It is being used increasingly for the processing of images [10]. It is based on the decomposition of the image into multiple channels, on the basis of their local frequency content, each with a different degree of resolution (i.e. multi-scale and multi-orientation components). The wavelet representation is an intermediate representation between the spatial representation and the Fourier. It is commonly implemented as a cascading series of high-pass and low-pass filters, based on the mother wavelet, applied sequentially to the low-pass image of the previous recursion. In practice, three or four recursions are sufficient. The conventional wavelet transform uses down-sampling and generates various frequency sub-bands less than the size of input image, while SWT generates frequency sub-band images of same resolution as the input LR image [14], [15]. Wavelet function decomposes an image into different sub-band images, namely low-low (LL), low- high (LH), high-low(HL), and high-high (HH). Another recent wavelet transforms which has been used in several image processing applications is stationary wavelet transform (SWT) [16], [17].

The second step in the proposed method (ie. image decomposition technique) uses SWT to decompose a low-resolution image into different sub-bands. and the wavelet function or "mother wavelet". Mother wavelet (t) undergoes translation and scaling operations to give self-similar wavelet families as given by Equation (3).

$$\psi a,b(t) = \frac{1}{\sqrt{a}} \psi \left(\frac{t-b}{a} \right), (a, b \epsilon R), a > 0 \qquad (3)$$

The wavelet transform decomposes the two images into low-high, high-low, high-high spatial frequency bands at different scales and the low-low band at the coarsest scale. The L-L band contains the average image information whereas the other bands contain directional information due to spatial orientation. Higher absolute values of wavelet coefficients in the high bands correspond to salient features such as edges or lines [18], [19].
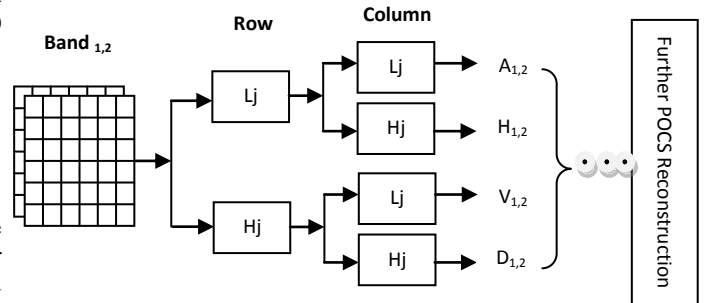

Fig 1. Stationary Wavelet Decomposition of two-dimensional bands

In Figure.1 Hj and Lj represent high-pass and low-pass filters at scale j , resulting from interleaved zero padding of filters.Band1,2 is the original images and the output of the scale j. A1,2 denotes the low frequency (LF) estimation1 after the stationary wavelet decomposition, while H1,2 , V1,2 and D1,2 denote the high frequency (HF) detailed information along the horizontal, vertical and diagonal directions, respectively. These sub-band images would have the same size as that of original image because no down- sampling is performed during the wavelet transformation [20]. In our approach we have used "Haar" wavelet to perform multi-layer stationary wavelet decomposition on the input 2D images. Mathematically, the wavelet decomposition of tow bands can be described by the following equations.

$$A_{j+1}(x, y) = \sum_{m,n} L[n]L[m]f(x, y)_j \left(2^{j+1}m - x, 2^{j+1}n - y \right) \quad (4)$$

$$H_{j+1}(x, y) = \sum_{m,n} L[n]L[m]f(x, y)_j \left(2^{j+1}m - x, 2^{j+1}n - y \right)(5)$$

$$V_{j+1}(x, y) = \sum_{m,n} H[n]L[m]f(x, y)_j \left(2^{j+1}m - x, 2^{j+1}n - y \right)(6)$$

$$D_{j+1}(x, y) = \sum_{m,n} H[n]H[m]f(x, y)_j \left(2^{j+1}m - x, 2^{j+1}n - y \right)(7)$$

SWT offers several advantages. First, each sub-band has the same size, so it is easier to get the relationship among the sub-bands. Second, the resolution can be retained since the original data is not decimated. Also at the same time the wavelet coefficients contain many redundant information which helps to distinguish the noise from feature [21]. Using SWT we have extracted horizontal, vertical and diagonal detail sub-matrices.

4. PROJECTION ONTO CONVEX SET (POCS)

super-resolution reconstruction process and interpolation are usually done by projection onto convex set (POCS) [22], [23]. (POCS) uses a priori knowledge about the imaging system in order to achieve the image restoration. The key to effectively apply POCS-based algorithms is to define the appropriate sets and compute the projections onto these sets until some criteria be achieved [24]. The POCS method giving a solution to the SR reconstruction problem was proposed in [25], [26], [27] and extended in [28]. Stark and Oskoui [29] firstly applied the POCS to super-resolution image reconstruction. Papa [30] proposed POCS algorithm based on particle swarm optimization (PSO), which used PSO to obtain the relaxation projection parameter. Eren [31] popularized Patti's method to the scene of multiple moving targets. Patti [32] proposed an image acquisition model of considering a variety of degraded factors including the camera movement, nonzero aperture time, blur caused by optical imaging components, sensor noise and any space-time sampling. Patti [33] presented a discrete image acquisition model and high-order interpolation method. Ogawa [34] presented POCS algorithm based on principal component analysis (PCA), which used PCA to image interpolation. Gho [35] applied POCS to the magnetic resonance images which utilized the low-pass and high-pass filter to improve the quality of the reconstructed image.

Let the motion information be provided. Then, a data consistency constraint set based on the acquisition model (section-2) can be defined for each pixel within each low resolution (LR) images. Generally, we first establish a degraded model to associate lower resolution images and the high-resolution image. The general model can be expressed as:

$$g_d(x, y, K) = \sum_{m,n} Q(m, n) h(x, y; m, n) + \varepsilon(x, y) \qquad (8)$$

where $g_d(x, y, K)$ is (LR) image, $Q(m, n)$ is an ideal (HR) image. $h(x, y; m, n)$ is the point spread function(PSF). $\varepsilon(x, y)$ represents the additive noise. The POCS is an iterative algorithm starting from a given initial estimation to obtain the efficient solution. Each kind of priori information restricts POCS solution to a closed convex set can be expressed as:

$$C_R(m, n, K) = \{Q(m.n): |r^{(Q)}(x, y, K)| \leq \delta_0\} \qquad (9)$$

where $C_R \in R$ denotes the ith constraint or a priori knowledge on component Q and C is the number of those sets. $Q(m, n)$ denoted discrete high resolution (HR) image. δ_0 represents the uncertainty that we have in the observation.

$$r^{(Q)}(x, y, K) = g_d(x, y, K) - \sum_{m,n} Q(m, n) h(m, n; x, y, k) \quad (10)$$

where the value $g_d(x, y, K)$ at each pixel (x, y) is constrained such that its associated residual It is bounded in magnitude by δ_0 for the set. Since the bound δ_0 is determined from the statistics of noise, the ideal image solution is a member of the set satisfying a certain statistical confidence. The projection of an arbitrary $Q(m, n)$ onto $C_R(m, n, K)$ is defined by [36].

$$P_R(x, y, k)[Q(m, n)] =$$
$$\begin{cases} Q(m, n) + \frac{(r^{(Q)}(x,y,K) - \delta_0).h(m,n;x,y,k)}{\sum_{m,n} h^2(m,n;x,y,k)}, r^{(Q)}(x, y, K) > \delta_0 \\ 0, -\delta_0 < r^{(Q)}(x, y, K) < \delta_0 \qquad (11) \\ Q(m, n) + \frac{(r^{(Q)}(x,y,K) + \delta_0).h(m,n;x,y,k)}{\sum_{m,n} h^2(m,n;x,y,k)}, r^{(Q)}(x, y, K) < -\delta_0 \end{cases}$$

Additional constraints such as bounded energy, positivity, and limited support may be utilized to improve the results. A generally utilized altitude constraint set is

$$P_A(x, y, k)[Q(m, n)] = \begin{cases} 0, Q(m, n) < 0 \\ Q(m, n), 0 \leq Q(m, n) \leq 255 \\ 255, Q(m, n) > 255 \end{cases} \qquad (12)$$

with amplitude bounds of 0,255 Let PA be a projection operator which simply clips the value of the operant so that the resulting value is between 0 and 255. The estimated SR image is obtained iteratively from all LR images, by cascading the two previously defined projection operators PA and PR.

$$Q_{i+1}(m, n) = P_A[P_R(x, y, k)[Q_i(m, n)]] \quad i = 1, 2, \ldots (13)$$

5. SWT CONSTRAINED POCS SUPER-RESOLUTION ALGORITHM

The third step of the proposed method is image reconstruction with a wavelet constrained POCS (SWT-POCS) technique. Instead of performing the POCS in the image domain itself, we update the wavelet coefficients in the A, H, V, and D bands using the neighboring frames of the reference frame [37]. The fundamental concept of the SWT- POCS is the interpolation of different SWT sub-bands [38]. The high frequency information are hidden in a group of low resolution images adjacent to the reference image. Based on this concept, we extend the existing image domain POCS algorithm and used SWT-based algorithm satisfying the POCS constraints [39].

Let $f(x, y), g(x, y) \in L2(R2)$ denote the low-resolution images, it can be expanded as a sum of an approximation component in the LL(D) band and three detail components in the LH(H), HL(V), and HH (D)bands.

$$f(x, y) = \sum_{k,l \in z} A_{k,l} \emptyset_{k,l}(x, y) + \sum_{k,l \in z} H_{k,l}(x, y) \psi^h_{k,l}(x, y)$$
$$+ \sum_{k,l \in z} V_{k,l}(x, y) \psi^v_{k,l}(x, y) + \sum_{k,l \in z} D_{k,l}(x, y) \psi^d_{k,l}(x, y) \quad (14)$$

where $\psi^h_{k,l}(x, y), \psi^v_{k,l}(x, y)$ and $\psi^d_{k,l}(x, y)$ are the (k, l) translated wavelets at the next coarse scale level that capture detail information in the horizontal, vertical and diagonal directions, respectively, and $\emptyset_{k,l}(x, y)$ is the (k, l) translated coarse scaling function; here the top equation denotes their corresponding functions used in the reconstruction process. The approximation and detail wavelet coefficients for (LR) images are given by

$$A1_{k,l} = \iint f(x, y) \emptyset_{k,l}(x, y) dxdy \qquad (15)$$

$$A2_{k,l} = \iint g(x, y) \emptyset_{k,l}(x, y) dxdy$$

$$H1_{k,l} = \iint f(x, y) \psi^h_{k,l}(x, y) dxdy \qquad (16)$$

$$H2_{k,l} = \iint g(x, y) \psi^h_{k,l}(x, y) dxdy$$

$$V1_{k,l} = \iint f(x, y) \psi^v_{k,l}(x, y) dxdy \qquad (17)$$

$$V2_{k,l} = \iint g(x, y) \psi^v_{k,l}(x, y) dxdy$$

$$D1_{k,l} = \iint f(x, y) \psi^d_{k,l}(x, y) dxd$$

$$D2_{k,l} = \iint g(x, y) \psi^d_{k,l}(x, y) dxdy \qquad (18)$$

Then, the defined convex set of low resolution images after performing stationary wavelet decomposition are given by:

$$C_{w,A} = \{f(x, y): \iint f(x, y) \emptyset_{k,l}(x, y) dxdy = S_{c,A}(g(x, y))\} \qquad (19)$$

$$C_{w,H} = \{f(x, y): \iint f(x, y) \psi^h_{k,l}(x, y) dxdy = S_{c,H}(g(x, y))\} \quad (20)$$

$$C_{w,V} = \{f(x, y): \iint f(x, y) \psi^v_{k,l}(x, y) dxdy = S_{c,V}(g(x, y))\} \quad (21)$$

$$C_{w,D} = \left\{ f(x,y) : \iint f(x,y)\, \psi^D_{k,l}(x,y)\,dxdy = S_{c,D}\big(g(x,y)\big) \right\} \quad (22)$$

where $C_{w,A}, C_{w,H}, C_{w,V}$ and $C_{w,D}$ are the convex set of wavelet coefficient and $S_{c,A}, S_{c,H}, S_{c,V}$ and $S_{c,D}$ denote an appropriate scaling of the second frame. The projection of an SWT coefficient onto $C_{w,A}, C_{w,H}, C_{w,V}$ and $C_{w,D}$ is defined by:

$$P_{w,A}[f(x,y)] = \sum_{k,l \in z} S_{c,A}\big(g(x,y)\big) \emptyset_{k,l}(x,y) \quad (23)$$

$$P_{w,H}[f(x,y)] = \sum_{k,l \in z} S_{c,H}\big(g(x,y)\big) \psi^H_{k,l}(x,y) \quad (24)$$

$$P_{w,V}[f(x,y)] = \sum_{k,l \in z} S_{c,V}\big(g(x,y)\big) \psi^V_{k,l}(x,y) \quad (25)$$

$$P_{w,D}[f(x,y)] = \sum_{k,l \in z} S_{c,D}\big(g(x,y)\big) \psi^D_{k,l}(x,y) \quad (26)$$

6. EGYPTSAT-1 DATA ACQUISITION AND STUDY AREA

The Egyptian satellite (Egyptsat-1) is the first earth observation satellite to Egypt. It was launched in April 2007, based on micro-satellite technology. The satellite is intended to image certain areas of ground and transmit its images to the ground data receiving station. The satellite consists of four payload subsystems; Multiband Earth Imager (MBEI), Middle IR Earth Imager (MIREI), Store and forward communication and command and data handling, Besides the extend observation capabilities (+/-35 degree) off-nadir cross-track pointing. It provided imaging in each of the modes Panchromatic (PAN), Multispectral (MS) and Infrared (IR). The characteristic of Egyptsat-1 data are as follows, according to A. Kolokolov et al [40]; the spatial resolutions of the MS and the PAN bands are 7.8 meters. The spatial resolution of the Mid-Infrared band is 39.5 meter [9], and the spectral resolutions are as shown in following Table (1).

Table .1 The Spectral resolutions of the Egyptsat-1 Data

Bands	Description	Wavelength (µm)
Band1	Green	0.51-0.59
Band2	Red	0.61-0.68
Band3	Near Infrared	0.80-0.89
Band4	Panchromatic	0.50-0.89
Band5	Mid Infrared	1.10-1.70

Due to malfunctioning of Egyptsat-1sensor, there is an irregular shift between band 1 and band 2 in some parts of its images. We are going to use this shift for the production of the super resolution image.

The study area is located in the North-East part of Cairo. Subsets of bands 1 and 2 of the Egyptsat-1 image covering this area and acquired on 31/5/2010 has been used in conducting our research, as shown in figure.2.

(a) Band.1   **(b) Band.2**

Fig 2. Egyptsat-1 Bands of the study area

7. METHODOLOGY

Step1: In this step, we transform the inconsistent sub-pixel shift into a consistent one for efficiently registering a set of LR images (Egyptsat-1 bands). It has been reported that band 1 and band 2 are misaligned, producing unregistered separate bands. The shift between these two bands is not constant along the whole image. In order to overcome the inconsistency of the sub-pixel shift through the LR bands. The main steps can be summarized as follows:

- Divide the input LR bands into small patches, T blocks of size M x M.

- Construct an error surface between these two bands by computing the shift in x, y directions for each block.

- Use joint frequency distribution analysis to determine an optimal x and y shift in order to maximize reconstruction accuracy while minimizing the overall shift error.

- Project one of the input LR bands into an empty grid shifted by delta x, y derived from the previous step.

Step2: Perform motion estimation (Δ_x, Δ_y and θ rotation) between the two bands using the method in [section_2]

Step3: Define set $C_R(m,n,k)$ according to Eq. (9), for each pixel site (m,n,k) where the motion information has been estimated.

Step4: Compute the blur $h(m,n;x,y,k)$ for every site (m,n,k) based on the set $C_R(m,n,k)$;

Step5: Compute the residual $r(.)$ according to Eq. (10);

Step6: Back-project the residual $r(.)$ using the projection $P_R(m,n,k)$ in Eq. (11);

Step7: The input LR images are decomposed using one level SWT (with bio-orthogonal) into different sub-bands. Three high frequency sub-bands contain horizontal, vertical and diagonal details of images.

Step8: Perform wavelet projection Pw using from Eq. (23) to Eq. (26);

Step9: Perform the amplitude projection PA using Eq. (12) for all wavelet sub-bands;

Step10: Finally, Reconstruct the SR output image using the inverse decomposition process (ISWT) to achieve a high-resolution output image after applying high pass filter, as explained in figure .3.
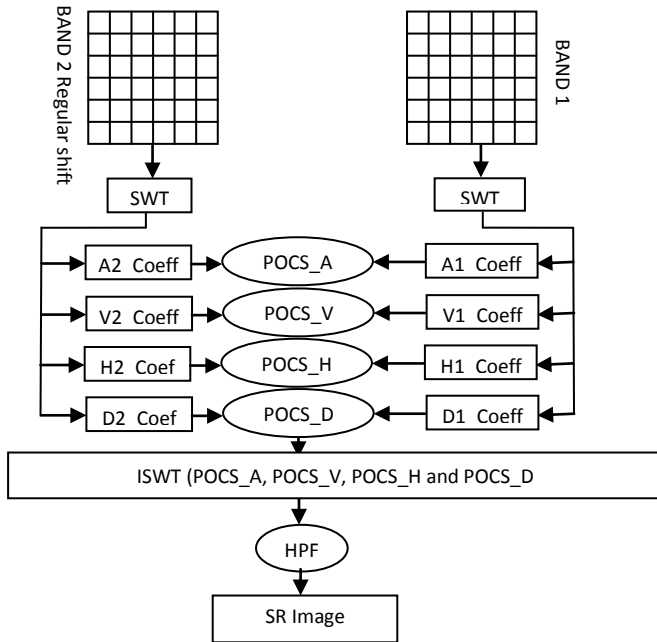
(a)   (b)

(c)   (d)

Fig 5. The output of the projection onto convex set Stationary wavelet coefficient ((a)Approximation;(b) Horizontal, ;(c) Vertical ;(d) Diagonal coefficients)

Fig 3. Block diagram of constructing a SR image of Egyptsat-1

8. RESULTS AND DISCUSSIONS

Applying step_1 yield LR band 2 with constant shift (0.3142, -0.5033 pixel and rotation -0.1) with respect to band 1. Figure.4 depicts the consistent sub-pixel shift.

To reconstruct a SR image (i.e. generate a single 4-meter pixel image from the previous two subsets 7.8-meter pixel bands), MATLAB implementations have been used. We applied the stationary wavelet decomposition algorithm to overcome the limitation of the orthogonal separable wavelet transform and used the projection onto convex set to perform the fusion between the wavelet coefficients. then, we reconstructed the SR output image using the inverse decomposition process(ISWT). The most detailed scale information of the image is located in the first wavelet planes; therefore, those are the fused(SWT-POCS) planes from the LR bands included in the resulting coefficient bands. Figure 5 shows the output of POCS of SWT coefficient (A, H, V and D). The high pass filter(HPF) used to improve the reconstructed SR images as shown in figure.6.
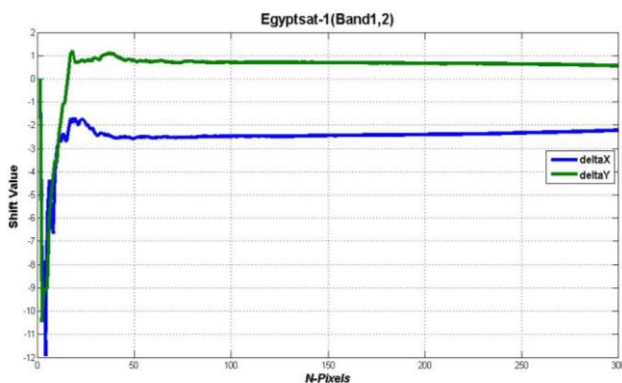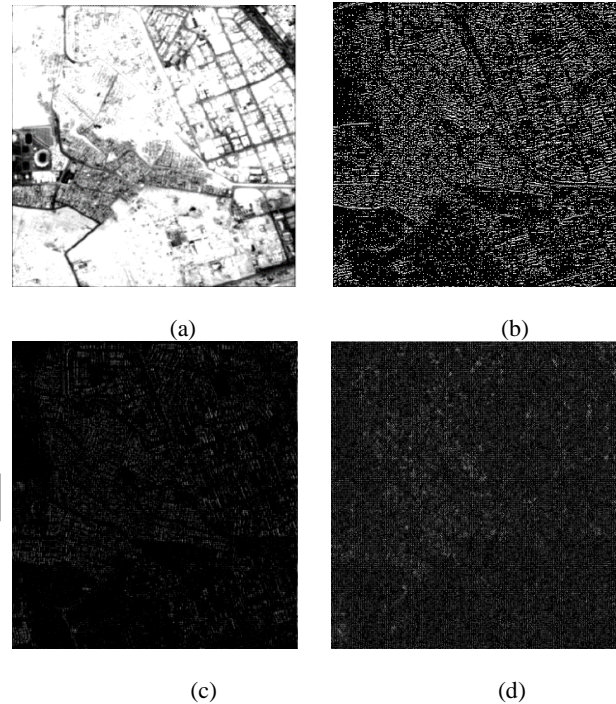

Fig 6. The high pass filter (HPF) of the SR reconstructed

9. EVALUATION CRITERIA

Currently, by visual comparison of the original LR images and the reconstructed SR output, it is easy to see that the spatial resolution of the SR image is clearly better than the original ones (i.e., increased). Thus, the proposed methodology and the used algorithms produce a significant improvement. Visually the SR image contains more information than the original bands. Objects as different as streets, buildings and green areas are clearly better shaped and/or recovered.

Besides the evident improvements shown in figure 6, we were also interested in an objective evaluation of the results. Therefore, we have used seven quantitative measures:

9.1 PEAK SIGNAL TO NOISE RATIO (PSNR)

PSNR is the ratio between the maximum possible power of a signal and the power of corrupting noise that affects the fidelity of its representation [41]. The PSNR measure is given by:

Fig 4. The Consistent Sub-Pixel Shifts of Egyptsat-1 (bands1,2)

$$PSNR(db) = 20\log \frac{255\sqrt{3MN}}{\sqrt{\sum_{i=1}^{M} \sum_{j=1}^{N} (B'(i,j) - B(i,j))^2}}$$

where B the perfect image, B′ the SR image to be assessed, i pixel row index, j pixel column index, M, N No. of row and column.

9.2 RMSE

RMSE has been widely used in the evaluation of image quality, and it is defined as

$$RMSE = \left(\frac{1}{MN} \sum_{i=1}^{M} \sum_{j=1}^{N} [I_R(i,j) - I_F(i,j)]^2 \right)^{\frac{1}{2}}$$

where I_R the perfect image, I_F the SR image to be assessed, i pixel row index, j pixel column index, M, N No. of row and column.

9.3 Entropy

Information entropy is an important indicator of the evaluation of images, and it is defined as:

$$H = - \sum_{i=0}^{l-1} P_i \log_2 P_i$$

where P_i is the probability of the pixel value i. Higher entropy indicates more information in the evaluated images.

9.4 Mutual Information(MI)

The mutual information MI_{AF} I_{AF} reflects the statistical dependence of two random variables as it measures the similarity of image intensity distribution between the source image A and the SR image F. It is obtained as follows:

$$MI_{AF} = \sum_{a,f} P_{AF}(a,f) \log \frac{P_{AF}(a,f)}{P_A(a)P_F(f)}$$

Where P_{AF} is the jointly normalized histogram of A and F. P_A and P_F are the normalized histogram of A and F. a, f represents the pixel value of the image A and F, respectively.

9.5 Objective Fusion Measure

The metric $Q^{AB/F}$ evaluates the amount of high frequency information transferred from the source images into the SR image. $Q^{AB/F}$ is defined as follows:

$$Q^{AB/F} = \frac{\sum_{n-1}^{N} \sum_{m-1}^{M} (Q^{AF}(n,m)W^A(n,m) + Q^{BF}(n,m)W^B(n,m))}{\sum_{n-1}^{N} \sum_{m-1}^{M} (W^A(n,m) + W^B(n,m))}$$

Where $Q^{AF}(n,m) = Q_g^{AF}(n,m) Q_\alpha^{AF}(n,m)$

$Q_g^{AF}(n,m)$ and $Q_\alpha^{AF}(n,m)$ are the edge strength and orientation preservation values respectively; n, m represents the pixel location; and N, M are the size of the images respectively. $Q^{BF}(n,m)$ is similar to $Q^{AF}(n,m)$. $W^A(n,m)$, $W^B(n,m)$ reflect the importance of $Q^{AF}(n,m)$ and $Q^{BF}(n,m)$, respectively. The dynamic range of $Q^{AB/F}$ is [0 1], and it should be as close to 1 as possible [42].

9.6 Average pixel intensity (API)

Average pixel intensity (API) measures an index of contrast and is given by:

$$API = \frac{\sum_{i=1}^{m} \sum_{j=1}^{n} f(i,j)}{m.n}$$

where $f(i,j)$ is pixel intensity at (i,j) and $m.n$ is the size of the image.

9.7 Standard Deviation (SD)

Standard deviation (SD) is the square root of the variance, which reflects the spread in data and is given by:

$$SD = \sqrt{\frac{\sum_{i=1}^{m} \sum_{j=1}^{n} (f(i,j) - F^-)^2}{m.n}}$$

where $f(i,j)$ is pixel intensity at (i,j) and $m.n$ is the size of the image. F^- is the mean of the image pixels.

In order to validate the proposed methodology, its performance was further quantitatively evaluated with some implemented commonly used SR methods in terms of all the previous quantitative measures. The implemented SR methods are; Iterative-Interpolation [43], Projection onto Convex Sets (POCS) [44], Iterated Back Projection [45], and Robust [46]. Their results are shown in figure 7 by zooming in subsections. the quantitative measures are calculated between the LR bands and the implemented SR methods to assess the amount of the information transferred, as shown in Table 2. Comparing the results, it is obvious that the proposed methodology has better values than all of the other methods. This indicates that the reconstructed SR image is strongly correlated with the source bands, confirms that the proposed methodology performs well in reconstructing the SR image, and proves that the objective evaluation results match with the visual effect significantly
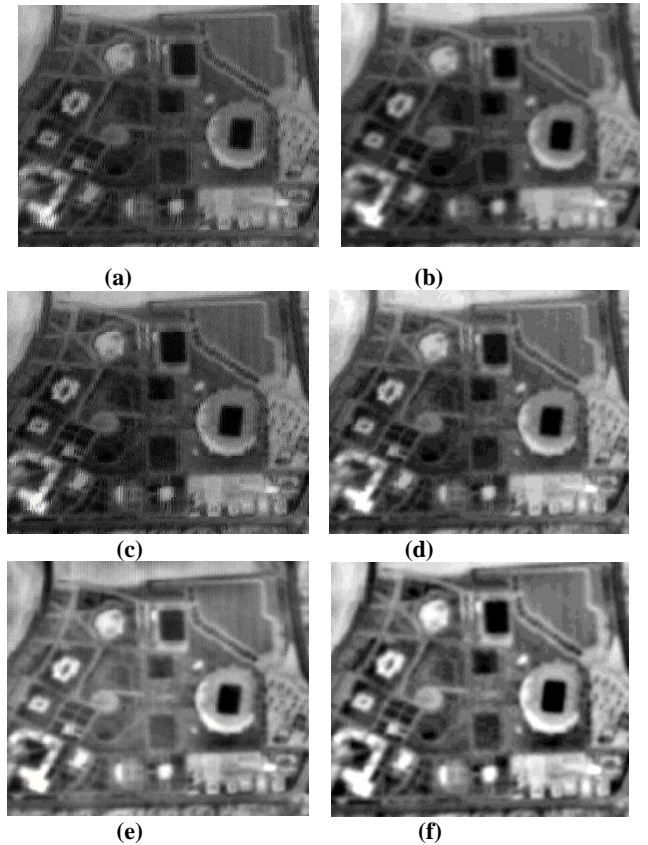

(a)　　　　　　(b)

(c)　　　　　　(d)

(e)　　　　　　(f)

Fig 7. Subsections of the SR images of the study area using different implemented SR methods; (a) Iterative-Interpolation, (b) POCS without WT, (c) Robust, (d) Normalized Convolution, (e) Iterated Back Projection, and (f) The Proposed Method

Table 2. The Results of Applying the Different Quantitative Measures on the Implemented SR Methods

	PSNR	RMSE	ENTROPY	MI_{AF}	$Q^{AB/F}$	API	SD
(a)	37.73	29.172	5.11	2.56	0.719	82.46	11.957
(b)	51.72	13.041	5.12	2.30	0.722	84.77	11.232
(c)	50.58	13.919	5.099	2.38	0.544	84.43	8.921
(d)	51.73	13.035	5.48	2.64	0.403	87.36	19.894
(e)	52.87	12.20	5.56	2.71	0.611	102.7	18.046
(f)	57.13	11.077	5.8331	2.92	0.825	105.2	21.8

10. CONCLUSIONS

Precise registration of images is the most important and challenging aspect of multi-frame image super-resolution (SR). In this paper, a proposed methodology that transforms the inconsistent sub-pixel shift of some Egyptsat-1 images to a reliable one to reconstruct a SR image. We demonstrate how this efficient methodology provides substantial accuracy. A SR reconstruction method based on the multi-resolution (POCS - SWT) decomposition SR was used. A core of the stationary wavelet decomposition algorithm and the Projection onto Convex Set techniques has been conducted. This paper aimed at recognition of objects with sizes approaching its limiting spatial resolution scale. For an objective evaluation of the proposed methodology, its performance was compared, in terms of different quantitative measures, with some implemented commonly used SR methods to verify its usefulness and effectiveness. The results of the implemented methods have shown that the proposed methodology yield better values compared to all of the other implemented ones. Therefore, this research demonstrates that the proposed methodology provides significant improvements in the SR results.

11. ACKNOWLEDGMENT

12. REFERENCES

[1] Nasr, A.H; Gh.S. El-Tawel; A.K. Helmy. "super resolution for egyptsat-1 images with erratic shift "Journal of Computer Science 10 (8): pp-1324-1335,ISSN:1549-3636, 2014

[2] S.A. Mohamed; A.K. Helmy; M.A. Fkirin; S.M. Badway" A Proposed Method to Measure Sub Pixel Shift in Egyptsat-1 Aliased Images"International Journal of Computer ApplicationsVolume 95– No. 10, June 2014

[3] T. Stathaki " Image Fusion: Algorithms and Applications". 1st ed. Amsterdam, The Netherlands: Elsevier. 2008

[4] Jifei Yu; Xinbo Gao; Dacheng Tao;Xuelong Li;Kaibing Zhang" A unified learning framework for single image super-resolution" IEEE transactions on neural networks and learning systems,volume:25 ,pp:780-792, issue:4, 2014

[5] Liu, Lixin; Bian, Hongyu; Shao, Guofeng" An effective wavelet-based scheme for multi-focus image fusion"IEEE International Conference on Mechatronics and Automation, pp:1720-1725, 2013

[6] Zitova B and Flusser J " Image Registration Methods: A Survey. Image and Vision Computing", 11(21), pp. 977–1000, 2003.

[7] Robinson D, Farsiu S and Milanfar P "Optimal Registration of Aliased Images Using Variable Projection with Application to Super-Resolution". The Computer Journal. 52, Issue 1, pp. 31–42, 2009.

[8] S.A. Mohamed; A.K. Helmi ; M.A. Fkirin; S.M. Badwai" Accuracy Analysis of Phase Correlation Shift Measurement Methods Applied to Egyptsat-1 Satellite" Radio Science Conference (NRSC), 2013 30th National ,ISBN 978-1-4673-6219-1,PP: 347-358,Cairo,Egypt ,16-18 April 2013

[9] S.A. Mohamed; A.K. Helmi ; M.A. Fkirin; S.M. Badwai, "Subpixel Accuracy Analysis of Phase Correlation Shift Measurement Methods Applied to Satellite Imagery"(IJACSA) International Journal of Advanced Computer Science and Applications, ISSN21565570,Vol. 3, No. 12, pp. 202-206, 2012.

[10] Starck J L and Pantin E"Multiscale maximum entropy image restoration". Vistas Astron. 40, pp. 563–569, 1996.

[11] Bernd Jähne, "Digital image processing" 6th Edition, ISBN 3-540-24035-7 Springer Berlin, Heidelberg, New York, 2005.

[12] Steven T. Karris, "Signals and Systems with MATLAB Applications, Second Edition", Orchard Publications, ISBN 0-9709511-8-3, 2003.

[13] Van Dewalle P"Super-resolution from Unregistered Aliased Images". Thèse No. 3591 école polytechnique fédérale de Lausanne pour l'obtention du grade de docteur ès sciences, 2006.

[14] Agrawal, Mayank Dash, Ratnakar" Image Resolution Enhancement Using Lifting Wavelet and Stationary Wavelet Transform" 2014 International Conference on Electronic Systems, Signal Processing and Computing Technologiespp- 322-325, 2014

[15] Deng, Juan Ban, Yifang Liu, Jinshuo Li, LiNiu, XinZou, Bin" Hierarchical Segmentation of Multitemporal RADARSAT-2 SAR Data Using Stationary Wavelet Transform and Algebraic Multigrid Method" IEEE Transactions on Geoscience and Remote Sensing,pp- 4353-4363,vol52 issue:7,2014

[16] J. E. Fowler, "The redundant discrete wavelet transform and additive noise,"Mississippi State ERC, Mississippi State University, Tech. Rep. MSSU-COE-ERC-04-04, Mar. 2004

[17] Demirel, Hasan; Anbarjafari, Gholamreza" IMAGE resolution enhancement by using discrete and stationary wavelet decomposition. IEEE transactions on image processing : a publication of the IEEE Signal Processing Society,2011

[18] Deepali A.Godse, Dattatraya S. Bormane "Wavelet based image fusion using pixel based maximum selection rule"International Journal of Engineering Science and Technology (IJEST), ISSN : 0975-5462, Vol. 3 No. 7 July 2011

[19] Gonzalo Pajares , Jesus Manuel de la Cruz "A wavelet-based image fusion tutorial" Pattern Recognition Society, 2004.

[20] G. P. Nason and B. W. Silverman-The stationary wavelet transform and some statistical applications in wavelet and statistics. In: Antoniadis A ed. Lecture Notes in Statistics. Berlin: Spinger Verlag, 281-299, 1995.

[21] Chaudhary, Manoj D. Upadhyay, Abhay B." Fusion of local and global features using Stationary Wavelet Transform for efficient Content Based Image Retrieval".2014 IEEE Students' Conference on Electrical, Electronics and Computer Science,pp-1-6,2014

[22] Pires, Rafael G. Pereira, Luis a. M. Mansano, Alex F. Papa, Joao P." A hybrid image restoration algorithm based on Projections Onto Convex Sets and Harmony Search" 2013 IEEE International Symposium on Circuits and Systems (ISCAS2013)pp-2824-2827,issue:3,2013

[23] Xi, Huiqin Xiao, Chuangbai Bian, Chunxiao." Edge Halo Reduction for Projections onto Convex Sets Super Resolution Image Reconstruction" 2012 International Conference on Digital Image Computing Techniques and Applications (DICTA),pp-1-7,2012

[24] H. Stark, Y. Yang, and Y. Yang, Vector Space Projections: A Numerical Approach to Signal and Image Processing, Neural Nets, and Optics. John Wiley & Sons, 1998

[25] D. C. Youlq "Generalized image restoration by the method of alternating orthogonal projections," IEEE Trans. Circuiis Syst., vol. CAS-25, pp.694-702, 1978.

[26] H. I. Trussell and M. R. Civanlar, "Feasible solution in signal restoration," IEEE Trans. Acousi., Speech, Signal Processing, vol. ASSP-32, pp. 201-212, 1984

[27] A.J. Patti, M. I. Sezan, and A. M Tekalp, "Superresolution Video ReconstNction with Arbitrary Sampling Lattices and Nonzero Aperture Time", IEEE Trans. Image Processing, vol. 6, no. 8, pp1646-1658, 1997

[28] A. Enis Cetin, Alican Bozkurt, Osman Gunay, Y. Hakan Habiboglu, Kivanc Kose, Ibrahim Onaran, R. A. Sevimli." Projections Onto Convex Sets (POCS) Based Optimization by Lifting" pp-4799 ,Issue:4 1st IEEE Global Conference on Signal and Information Processing (GLOBALSIP)", 2013

[29] H. Stark, P. Oskoui, "High-resolution image recovery from image plane arrays using convex projections," Journal of the Optical Society of America A. vol. 6, pp. 1715-1726, 1989.

[30] J. P. Papa, L. M. G. Fonseca, and L. A. S. de Carvalho, "Projections onto convex sets through particle swarm optimization and its application for remote sensing image restoration," Pattern Recognition Letters. vol. 31, pp. 1876-1886, 2010

[31] P. E. Eren, M. I. Sezan, and A. M. Tekalp, "Robust, object-based high- resolution image reconstruction from low-resolution video," IEEE Transactions on Image Processing. vol.10, pp. 1446-1451, 1997

[32] J. Patti, M. I. Sezan, and A. M. Tekalp, "Super-resolution video re- construction with arbitrary sampling lattices and nonzero aperture time," IEEE Transactions on Image Processing. vol.8, pp.1064-1076, 1997

[33] A. J. Patti, Y. Altunbasak, "Artifact reduction for set theoretic super resolution image reconstruction with edge adaptive constraints and higher-order interpolants," IEEE Transactions on Image Processing. vol. 10, pp. 179-186, 2001.

[34] T. Ogawa, M. Haseyama, "Missing intensity interpolation using a kernel PCA-based POCS algorithm and its applications," IEEE Transactions on Image Processing. vol. 20, pp. 417-432, 2011

[35] S. Gho, C. Liu, and D. Kim. "Application of low-pass & high-pass reconstruction for improving the performance of the POCS based algorithm,"in 2011 IEEE 54th International Midwest Symposium on Circuits and Systems (MWSCAS). Korea: Seoul, pp. 1-3, 2011

[36] Huiqin Xi,Xiao, Chuangbai Xiao, Chunxiao Bian"Edge Halo Reduction for Projections onto Convex Sets Super Resolution Image Reconstruction"2012 International Conference on Digital Image Computing Techniques and Applications (DICTA) ,pp:1-7 , 2012

[37] Nelson.l;Avideh zakhor" Constructing a Multivalued Representation for View Synthesis" International Journal of Computer Vision, Volume 45 Issue 2, Pages 157 - 190, November2001

[38] Marcia L. S. Aguena, Nelson D. A. . Mascarenhas" Multispectral image data fusion using POCS and super-resolution" Volume 102 Issue 2,Pages 178-187. Elsevier Science Inc. New York, May 2006.

[39] Hsu, J.T; Sclabassi, R.J." A wavelet constrained POCS supper-resolution algorithm for high resolution image reconstruction from video sequence" International Conference on Neural Networks and Signal Processing,vol:2,pp:1266-1269, Proceedings of the 2003

[40] A. Kolokolov.,G. Tarasov.,S. Medvednikone.,V. Gladilin.,"Egyptsat-1 satellite specification" NARSS technology transfer documents., Issue 3, pp13-26, 2006.

[41] M .Chandana,S. Amutha, and Naveen Kumar, " A Hybrid Multi-focus Medical Image Fusion Based on Wavelet Transform". International Journal of Research and Reviews in Computer Science (IJRRCS) Vol. 2, No. 4, ISSN: 2079-2557, August 2011

[42] C.S. Xydeas and V. Petrovid" Objective image fusion performance measure" ELECTRONICS LETTERS 17th February 2000 Vol. 36 No. 4

[43] Bannore V "Iterative-interpolation super-resolution image reconstruction: A computationally efficient technique. Springer, Berlin, 2009.

[44] Panda S S, Prasad M S R S, and Jena G "POCS based Super-resolution image reconstruction using an adaptive regularization parameter". IJCSI International Journal of Computer Science, 8, Issue 5, No. 2, 2011.

[45] Irani M and Peleg S "Improving resolution by image registration. Graphical Models and Image Processing", 53, pp. 231-239, 1991.

[46] Zomet A, Rav-Acha A and Peleg S "Robust Super-Resolution". Proc. of the International Conference on Computer Vision and Pattern Recognition (CVPR), 2001.